Robustness Analysis of Mixed Product Run-to-Run Control for Semiconductor Process Based on ODOB Control Structure

An-Chen Lee, Jeng-Haur Horng, Tzu-Wei Kuo, and Nan-Hung Chou

***Abstract*—In this paper, we propose a unified framework for the mixed-product run-to-run (RtR) controller, which is called the output disturbance observer (ODOB) structure. Many mixed-product RtR controllers, such as product-based exponentially weighted moving average (PB-EWMA) threaded predictor corrector controller (t-PCC), cycle forecasting EWMA (CF-EWMA), and combined product and tool disturbance estimator (CPTDE), can fit in this framework. The relations of the above-mentioned controllers and the ODOB controller are discussed. Furthermore, based on the ODOB structure, we analyze the robust stable conditions and provide a systematic method for obtaining the optimal parameters that guarantee the optimal nominal performance under the robust stability. The simulation cases show that the output performances of PB-EWMA, t-PCC, CF-EWMA, and CPTDE controllers are improved by using the optimal weights obtained from the proposed approach.**

***Index Terms*—Disturbance observer, uncertainty, mixed product, robust stability, run-to-run**

I. Introduction

In THE past, Box and Jenkins [1] introduced the exponentially weighted moving average (EWMA) statistic, a minimum mean square error controller for the process disturbance following an integrated moving average (1,1), IMA(1,1), time series process. Sachs *et al*. [2] proposed the Run-to-Run (RtR) control scheme based on the EWMA statistic. They used the linear static models to a design feedback-based RtR controller and used the EWMA statistic as an estimate of the process. However, if there exists severe tool aging or the process drifts, the EWMA controller could not compensate for the steady drifts but produce an offset in the process output. For overcoming the offset caused by the EWMA controller, a predictor corrector controller (PCC) [3] and a double EWMA controller (dEWMA controller) [4] were developed. Actually, the EWMA, the PCC and the dEWMA controllers can be represented in terms of the internal model control (IMC) structure [3], [5]. Castillo [6] studied the property of PCC controller, and the weights of PCC controller were calculated by minimizing a performance trade-off between long-run and transient responses. Lee *et al*. [7] presented a unified framework called the output disturbance observer (ODOB) structure for EWMA, dEWMA and PCC controllers. The work enhances insight into the well-known established algorithms, and contributes to better understanding of how these algorithms operate and why they can be used successfully in practical application.

For mixed product process control schemes, Ma *et al*. [8] proposed a dynamic analysis of variance (ANOVA) approach to deal with RtR control of a high mixed operation. The conditions of different tools and products are identified based on the ANOVA analysis of the system output. A dynamic term in the form of autoregressive integrated moving average (ARIMA) disturbance model is included in the process model to characterize the RtR disturbances. Firth *et al*. [9] proposed the method Just-in-time Adaptive Disturbance Estimation (JADE) to deal with the variation of products in mixed semiconductor processes. They broke down the disturbances into contributions of current product and current tool. Zheng [10] brought up a mixed product process by EWMA control theory and separated it into tool-based EWMA (TB-EWMA) control and product-based EWMA (PB-EWMA) control. According to Zheng's work, PB-EWMA control is the better control scheme to deal with the problems in the mixed product situation. Ma *et al*. [11] studied the effect of production frequency on optimal weights tuning of threaded EWMA (t-EWMA), also called PB-EWMA, controller in a high-mixed production. Ai *et al*. [12] proposed a cycle forecasting EWMA (CF-EWMA) approach to deal with the large deviations in the first few runs of each cycle under drift disturbance. Ai *et al*. [13] proposed a drift compensatory approach which is based on threaded PCC (t-PCC) controller to deal with large deviations at the beginning runs of specific cycle process in a mixed production. Lee *et al*. [14] proposed a combined product and tool disturbance estimator (CPTDE) which combines threaded dEWMA controller and drift compensation scheme to adaptively estimate the disturbance for a mixed product situation in semiconductor processes.

Stability analysis for the mixed product situation is rarely studied in the past. Few papers have investigated the special

Manuscript received July 28, 2013; revised November 14, 2013; accepted January 21, 2014. Date of publication January 28, 2014; date of current version May 1, 2014. This work was supported by the National Science Council of Taiwan, Republic of China, under Grant NSC 100-2221-E-009-063-MY2 and Grant NSC 102-2218-E-150-001.

A.-C. Lee, T.-W. Kuo, and N.-H. Chou are with the Department of Mechanical Engineering, National Chiao Tung University, Hsinchu 300, Taiwan (e-mail: aclee@mail.nctu.edu.tw; ypk.me94g@nctu.edu.tw; hoho80265@gmail.com).

J.-H. Horng is with the Department of Power Mechanical Engineering, National Formosa University, Yunlin 632, Taiwan (e-mail: jhhorng@gmail.com.tw).

Color versions of one or more of the figures in this paper are available online at http://ieeexplore.ieee.org.

Digital Object Identifier 10.1109/TSM.2014.2303206

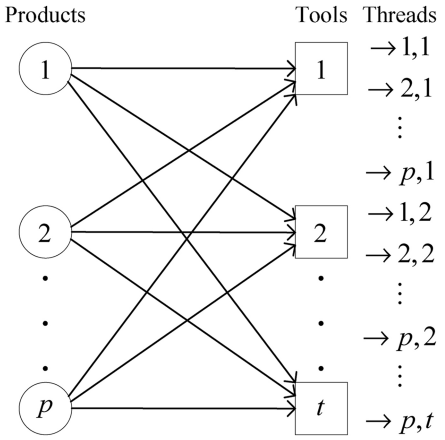

Fig. 1. Mixed product manufacturing process.

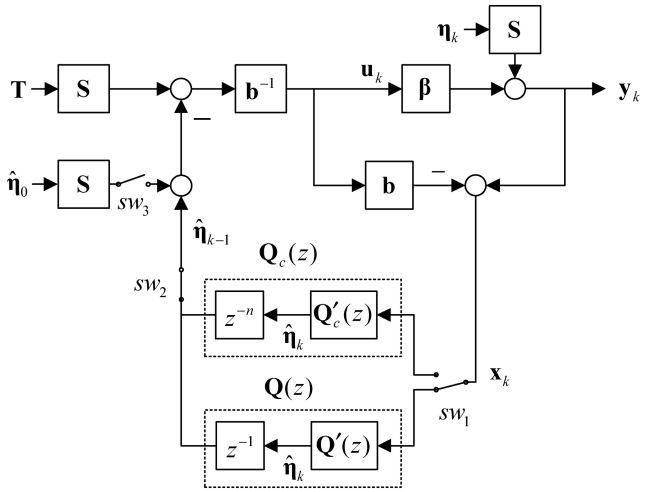

Fig. 2. The ODOB structure applied to the mixed product process.

stability conditions, for example, under regular (cycle) production situation with specific drift disturbances, i.e., IMA(1,1) with drift [10], [12]–[14]. Others have studied the selection of weights for mixed product process [10] and [14]. However, the analytic methods of those papers are not feasible for the non-regular production situation; furthermore, the uncertainty bound of the mixed product process is not considered in their approaches. In this paper, following the previous work of [7], we propose a unified framework for the mixed-product Run-to-Run (RtR) controller, i.e., ODOB structure. Many above-mentioned mixed-product RtR controllers, such as PB-EWMA, t-PCC, CF-EWMA and CPTDE, can be fit with this framework. With mild assumptions, we can analyze the robust stable conditions and provide a systematic method for obtaining the optimal parameters which guarantee the optimal nominal performance under the robust stability.

The rest of this paper is organized as follows. Section II illustrates the mixed product ODOB structure and the relations of the parameters among the PB-EWMA, t-PCC, CF-EWMA, CPTDE and the ODOB controller are discussed. In Section III, one analyzes the robust stability for mixed product RtR controllers using the ODOB control structure. Section IV demonstrates the procedure to design the optimal parameters of the mixed product ODOB under deterministic trend (DT) and ARIMA(1,1,1) disturbances. Section V demonstrates the advantage of the proposed method in improving the performance of the mixed product using simulation examples in the literature and the final section draws the conclusion.

II. ODOB Structure Applied to Mixed Product RtR Control

A. ODOB Structure

In this section, one will demonstrate the thread concept and extend the ODOB control structure [7] in the mixed product processes. Fig. 1 illustrates a "mixed product" manufacturing situation which contains p products and t tools. The "thread" is a specific production combination of product and tool, e.g. the thread 1,1 denotes product 1 and tool 1 manufacturing combination.

Based on the manufacturing processes as mentioned above, the linear model of mixed product processes can be represented as follows:

$$\boldsymbol{y_k = \beta u_k + \eta_k} \tag{1}$$

where $\mathbf{y}_k = \left[y_{1,1,k}, \cdots, y_{p,t,k}\right]^T \in \mathbb{R}^{(p\times t)\times 1}$ denotes process output, $\boldsymbol{\beta} = diag\left\{\beta_{1,1}, \cdots, \beta_{p,t}\right\} \in \mathbb{R}^{(p\times t)\times(p\times t)}$ denotes process gain, $\mathbf{u}_k = \left[u_{1,1,k}, \cdots, u_{p,t,k}\right]^T \in \mathbb{R}^{(p\times t)\times 1}$ denotes process input and $\boldsymbol{\eta}_k = \left[\eta_{1,1,k}, \cdots, \eta_{p,t,k}\right]^T \in \mathbb{R}^{(p\times t)\times 1}$ includes process intercept, drift and disturbance. The corresponding block diagram of the mixed product ODOB can be represented as Fig. 2, where $\mathbf{b} = diag\left\{b_{1,1}, \cdots, b_{p,t}\right\} \in \mathbb{R}^{(p\times t)\times(p\times t)}$ denotes the model gain, $\mathbf{T} = \left[T_{1,1} \cdots T_{p,t}\right]^T \in \mathbb{R}^{(p\times t)\times 1}$ denotes the process target, $\hat{\boldsymbol{\eta}}_k = \left[\hat{\eta}_{1,1,k} \cdots \hat{\eta}_{p,t,k}\right]^T \in \mathbb{R}^{(p\times t)\times 1}$ denotes the estimation of process intercept (or "intercept and drift" for t-PCC and CPTDE controllers), $\hat{\boldsymbol{\eta}}_0 = \left[\hat{\eta}_{1,1,0} \cdots \hat{\eta}_{p,t,0}\right]^T \in \mathbb{R}^{(p\times t)\times 1}$ denotes the initial value of process intercept (or "intercept and drift" for t-PCC and CPTDE controllers), $\mathbf{Q}(z) = diag\left\{Q_{1,1}(z), \cdots, Q_{p,t}(z)\right\} \in \mathbb{R}^{(p\times t)\times(p\times t)}$ denotes the low-pass filter (Q-filter) when the process thread keeps on processing, and $\mathbf{Q}_c(z) = diag\left\{Q_{c,1,1}(z), \cdots, Q_{c,p,t}(z)\right\} \in \mathbb{R}^{(p\times t)\times(p\times t)}$ denotes the transient low-pass filter when the process thread has been exchanged. The following cases illustrate the operation procedure of mixed product ODOB control structure.

Case 1: Initial values By referring to Fig. 2, for each thread enters into the process for the first time, the initial values of process intercept (or "intercept and drift") of these threads are given by $\hat{\boldsymbol{\eta}}_0$. At this moment, the sw_2 turns off and the sw_3 turns on. Except for the first run of each thread, the sw_2 turns on and sw_3 turns off all the time.

Case 2: For the thread keeping on processing The sw_1 will switch to $\mathbf{Q}(z)$ and the sw_2 and sw_3 will turn on and off, respectively, if the thread keeps on processing. Furthermore, the notion $\mathbf{S}$ provides an index for the mixed product ODOB structure to recognize which thread is processing. For example,

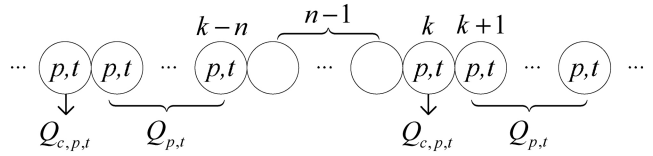

Fig. 3. The mixed product schedule.

when the thread 2,1 enters into the processing, $\mathbf{S} = diag\{0, 1, 0, \cdots, 0\} \in \mathbb{R}^{(p\times t)\times(p\times t)}$.

Case 3: Thread exchange (e.g. thread *p,t* is exchanged with thread 1,1) When the thread is exchanged from the other to the thread 1,1, the sw_2 turns on, and the sw_1 switch to $\mathbf{Q}_c(z)$ for activating the element $Q_{c,1,1}(z)$. If the next run is still the thread 1,1, the sw_1 will switch to $\mathbf{Q}(z)$ for activating the element $Q_{1,1}(z)$. However, the sw_1 will keep at $\mathbf{Q}_c(z)$ for activating the element $Q_{c,p,t}(z)$ if the thread 1,1 is exchanged immediately to the thread *p,t* in the next run.

B. RtR controllers represented as the ODOB control structure

This section will briefly review the PB-EWMA [10], t-PCC [13], CF-EWMA [12] and CPTDE [14] filter structures in the mixed product processes and discuss the relationship between those filters as mentioned above and the *Q*-filter of mixed product ODOB.

For illustrating the relationship more clearly, one considers the case of the multi-products entering into one tool case (as shown in Fig. 3). Each product can be considered as individual thread in this case, and the break products denote other threads in this process schedule.

1) PB-EWMA filter:

a) For thread p,t keeping on processing: When the thread *p,t* keeps on processing, the process intercept, $\hat{\eta}_{p,t,k+1}$, is calculated by

$$\hat{\eta}_{p,t,k+1} = \lambda_{p,t}x_{p,t,k+1} + \left(1-\lambda_{p,t}\right)\hat{\eta}_{p,t,k} \tag{2}$$

where $x_{p,t,k+1} = y_{p,t,k+1} - bu_{p,t,k+1}$ and $\lambda_{p,t}$ is the PB-EWMA weight ($0 < \lambda_{p,t} \le 1$). Equation (2) can be represented as a transfer function form as follows:

$$Q_{E,p,t}(z) = \frac{\hat{\eta}_{p,t}(z)}{X_{p,t}(z)}\cdot z^{-1} = \frac{\lambda_{p,t}}{z-\left(1-\lambda_{p,t}\right)} \tag{3}$$

Thus, the PB-EWMA filter can be represented as $\mathbf{Q}$ form in the mixed product ODOB structure in Fig. 2:

$$\mathbf{Q}(z) = diag\left\{Q_{E,1,1}, \cdots, Q_{E,p,t}\right\} \in \mathbb{R}^{(p\times t)\times(p\times t)}$$

b) Thread exchange: When the thread is exchanged from the other to the thread *p,t* on run *k*, assuming the other thread has been processed $n-1$ runs, the intercept estimation, $\hat{\eta}_{p,t,k}$, can be calculated by:

$$\hat{\eta}_{p,t,k} = \lambda_{p,t}x_{p,t,k} + \left(1-\lambda_{p,t}\right)\hat{\eta}_{p,t,k-n} \tag{4}$$

Taking z-transform in (4) to yield

$$Q_{E_c,p,t}(z) = \frac{\hat{\eta}_{p,t}(z)}{X_{p,t}(z)}\cdot z^{-n} = \frac{\lambda_{p,t}}{z^n-\left(1-\lambda_{p,t}\right)} \tag{5}$$

Hence, $\mathbf{Q}_c$ can be represented as:

$$\mathbf{Q}_c = diag\left\{Q_{E_c,1,1}, \cdots, Q_{E_c,p,t}\right\} \in \mathbb{R}^{(p\times t)\times(p\times t)}$$

2) t-PCC filter:

a) For the thread p,t keeping on processing: The intercept and drift estimation of the t-PCC filter can be expressed as:

$$\begin{cases} \hat{\eta}_{p,t,k+1} = \hat{a}_{p,t,k+1} + \hat{d}_{p,t,k+1} \\ \hat{a}_{p,t,k+1} = \lambda_{p,t}\left(x_{p,t,k+1}\right) + \left(1-\lambda_{p,t}\right)\hat{a}_{p,t,k} \\ \hat{d}_{p,t,k+1} = w_{p,t}\left(x_{p,t,k+1} - \hat{a}_{p,t,k}\right) + \left(1-w_{p,t}\right)\hat{d}_{p,t,k} \end{cases} \tag{6}$$

where $\lambda_{p,t}$ and $w_{p,t}$ are the weights of t-PCC ($0 < \lambda_{p,t} \le 1, 0 < w_{p,t} \le 1$). Taking z-transform in (6) to yield:

$$\begin{aligned} Q_{P,p,t}(z) &= \frac{\hat{\eta}_{p,t}}{X_{p,t}}z^{-1} \\ &= \frac{\left(\lambda_{p,t}+w_{p,t}\right)z + \left(\lambda_{p,t}w_{p,t} - \lambda_{p,t} - w_{p,t}\right)}{z^2 + \left(\lambda_{p,t}+w_{p,t}-2\right)z + \left(1-\lambda_{p,t}-w_{p,t}-\lambda_{p,t}w_{p,t}\right)} \end{aligned} \tag{7}$$

and $\mathbf{Q} = diag\left\{Q_{P,1,1}, \cdots, Q_{P,p,t}\right\} \in \mathbb{R}^{(p\times t)\times(p\times t)}$

b) Thread exchange: Same as the case of PB-EWMA thread exchange, the intercept and drift estimation of t-PCC filter can be obtained by:

$$\begin{cases} \hat{\eta}_{p,t,k} = \hat{a}_{p,t,k} + \hat{d}_{p,t,k} \\ \hat{a}_{p,t,k} = \lambda_{p,t}\left(x_{p,t,k}\right) + \left(1-\lambda_{p,t}\right)\hat{a}_{p,t,k-n} \\ \hat{d}_{p,t,k} = w_{p,t}\left(x_{p,t,k} - \hat{a}_{p,t,k-n}\right) + \left(1-w_{p,t}\right)\hat{d}_{p,t,k-n} \end{cases} \tag{8}$$

Taking z-transform in (8) to obtain:

$$\begin{aligned} Q_{P_c,p,t}(z) &= \frac{\hat{\eta}_{p,t}(z)}{X_{p,t}(z)}\cdot z^{-n} \\ &= \frac{\left(\lambda_{p,t}+w_{p,t}\right)z^n + \left(\lambda_{p,t}w_{p,t} - \lambda_{p,t} - w_{p,t}\right)}{z^{2n} + \left(\lambda_{p,t}+w_{p,t}-2\right)z^n + \left(1-\lambda_{p,t}-w_{p,t}-\lambda_{p,t}w_{p,t}\right)} \end{aligned} \tag{9}$$

and $\mathbf{Q}_c = diag\left\{Q_{P_c,1,1}, \cdots, Q_{P_c,p,t}\right\} \in \mathbb{R}^{(p\times t)\times(p\times t)}$

3) CF-EWMA:

a) For the thread p,t keeping on processing: According to the CF-EWMA algorithm [12], the intercept estimation, $\hat{\eta}_{p,t,k}$, can be obtained by (2):

$$\hat{\eta}_{p,t,k+1} = \lambda_{p,t}x_{p,t,k+1} + \left(1-\lambda_{p,t}\right)\hat{\eta}_{p,t,k}$$

The corresponding Q-filter can be represented as:

$$Q_{CF,p,t}(z) = \frac{\hat{\eta}_{p,t}(z)}{X_{p,t}(z)}\cdot z^{-1} = \frac{\lambda_{p,t}}{z-\left(1-\lambda_{p,t}\right)} \tag{10}$$

and $\mathbf{Q}(z) = diag\left\{Q_{CF,1,1}, \cdots, Q_{CF,p,t}\right\} \in \mathbb{R}^{(p\times t)\times(p\times t)}$ which are the same as PB-EWMA.

b) Thread exchange: Based on the CF-EWMA algorithm, the intercept estimation $\hat{\eta}_{p,t,k}$ can be calculated by:

$$\begin{aligned} \hat{\eta}_{p,t,k} &= \lambda_{p,t}\left(\bar{y}_{p,t} - T_{p,t}\right)n + \hat{\eta}_{p,t,k-n} \\ &= \lambda_{p,t}x'_{p,t}n + \hat{\eta}_{p,t,k-n} \end{aligned} \tag{11}$$

where $\bar{y}_{p,t}$ is output average of the thread *p,t* at the last production cycle, and $x'_{p,t} = \bar{y}_{p,t} - T_{p,t}$. Taking z-transform in (11) to yield:

$$\begin{aligned} Q_{CF_c,p,t}(z) &= \frac{\hat{\eta}_{p,t}(z)}{X'_{p,t}(z)}\cdot z^{-n} \\ &= \frac{\psi_{p,t}\left(z^{m-1}+z^{m-2}+\cdots+z\right)}{z^n\left[z^{n+m-1}-z^{m-1}+\psi_{p,t}\left(z^{m-2}+z^{m-3}+\cdots+1\right)\right]} \end{aligned} \tag{12}$$

where $\psi_{p,t} = \frac{n\lambda_{p,t}}{m-1}$, m is the number of the thread p,t at the last production cycle. Hence,

$$\mathbf{Q}_c = diag\left\{Q_{CF_c,1,1}, \cdots, Q_{CF_c,p,t}\right\} \in \mathbb{R}^{(p\times t)\times(p\times t)}.$$

4) CPTDE:

The CPTDE scheme which is originated from dEWMA has almost the same structure as that of t-PCC when the thread p,t keeps on processing.

a) For thread p,t keeping on processing: the process intercept and drift are estimated by CPTDE filter can be represented as follows:

$$\begin{cases} \hat{\eta}_{p,t,k+1} = \hat{a}_{p,t,k+1} + \hat{d}_{p,t,k+1} \\ \hat{a}_{p,t,k+1} = \lambda_{p,t}\left(x_{p,t,k+1}\right) + \left(1-\lambda_{p,t}\right)\left(\hat{a}_{p,t,k} + \hat{d}_{p,t,k}\right) \\ \hat{d}_{p,t,k+1} = w_{p,t}\left(x_{p,t,k+1} - \hat{a}_{p,t,k}\right) + \left(1-w_{p,t}\right)\hat{d}_{p,t,k} \end{cases} \quad (13)$$

Taking z-transform in (13) to yield:

$$\begin{aligned} Q_{CPTDE,p,t}(z) &= \frac{\hat{\eta}_{p,t}(z)}{X_{p,t}(z)} z^{-1} \\ &= \frac{\left(\lambda_{p,t} + w_{p,t}\right) z - \lambda_{p,t}}{z^2 + \left(\lambda_{p,t} + w_{p,t} - 2\right) z + \left(1-\lambda_{p,t}\right)} \end{aligned} \quad (14)$$

and $\mathbf{Q} = diag\left\{Q_{CPTDE,1,1}, \cdots, Q_{CPTDE,p,t}\right\} \in \mathbb{R}^{(p\times t)\times(p\times t)}$

b) Thread exchange: Based on the CPTDE algorithm, the intercept and drift estimation can be calculated by:

$$\begin{cases} \hat{\eta}_{p,t,k}=\hat{a}_{p,t,k}+n\hat{d}_{p,t,k} \\ \hat{a}_{p,t,k}=\hat{a}_{p,t,k-n}+n\hat{d}_{p,t,k-n}+\lambda_{p,t} \\ \left(y_{p,t,k}-b_{p,t}u_{p,t,k}-\hat{a}_{p,t,k-n}-n\hat{d}_{p,t,k-n}\right) \\ \hat{d}_{p,t,k}=\hat{d}_{p,t,k-n}+w_{p,t}\left(y_{p,t,k}-b_{p,t}u_{p,t,k}-\hat{a}_{p,t,k-n}-n\hat{d}_{p,t,k-n}\right) \end{cases} \quad (15)$$

Taking z-transform in (15) to yield:

$$\begin{aligned} Q_{CPTDE_c,p,t}(z) &= \frac{\hat{\eta}_{p,t}(z)}{X_{p,t}(z)} z^{-n} \\ &= \frac{\left(\lambda_{p,t} + nw_{p,t}\right) z^n - \lambda_{p,t}}{z^{2n} + \left(\lambda_{p,t} + nw_{p,t} - 2\right) z^n + \left(1-\lambda_{p,t}\right)} \end{aligned} \quad (16)$$

and $\mathbf{Q}_c = diag\left\{Q_{CPTDE_c,1,1}, \cdots, Q_{CPTDE_c,p,t}\right\} \in \mathbb{R}^{(p\times t)\times(p\times t)}$.

In summary, for the thread p,t, the filter structure relationships among PB-EWMA, t-PCC, CF-EWMA, CPTDE with $\mathbf{Q}$ and $\mathbf{Q}_c$ filters are listed in Tables I and II, respectively.

III. Robustness Analysis of the ODOB Control Structure

The model mismatch exists because the experimental data are insufficient to establish the process model. Actually, the semiconductor process condition always changes with time and the system modeling uncertainty affect the system stability and performance. Therefore, the actual plant $\boldsymbol{\beta}$ is not always equivalent to the nominal plant $\mathbf{b}$ in the process. The model mismatch ξ has been defined as $\xi = \boldsymbol{\beta} b^{-1}$ in the past. Here, the relation of the actual and the nominal plant is defined as

$$\boldsymbol{\beta} = \mathbf{b} + \Delta \quad (17)$$

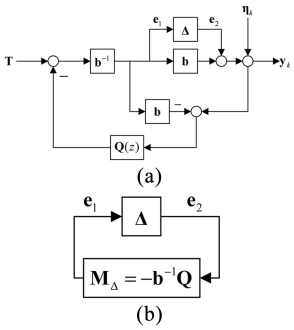

Fig. 4. (a) The ODOB structure with additive modeling uncertainty [7], (b) The standard $\Delta - \mathbf{M}$ loop for robust stability analysis of ODOB structure [7].

where Δ is the modeling uncertainty in terms of the additive uncertainty of the process model. The relation between the modeling uncertainty and the model mismatch is $|\Delta| = |(\xi - 1)|\,\mathbf{b}$. The ODOB structure with additive modeling uncertainty is shown in Fig. 4.(a), which can be further merged into a standard $\Delta - \mathbf{M}$ loop of the small gain theorem [15] which is usually used to obtain robust stability in robust control and shown in Fig. 4.(b).

According to the small gain theorem, suppose $\mathbf{M} \in RH_\infty$, then the interconnected system is well-posed and internally stable for all $\Delta \in RH_\infty$ with

$$\|\Delta\|_\infty \|\mathbf{M}\|_\infty \le 1 \quad (18)$$

where $\mathbf{M}$ is the transfer function from $\mathbf{e}_2$ to $\mathbf{e}_1$, or

$$\mathbf{M} = -\mathbf{b}^{-1}\mathbf{Q} \quad (19)$$

The transfer function $\mathbf{M}$ is related to the nominal plant $\mathbf{b}$ and the Q-filter. According to the assumption of the small gain theorem ($\mathbf{M} \in RH_\infty$), the Q-filter needs to be stable since $\mathbf{b}$ is just a constant gain.

If a bound of the possible modeling uncertainty Δ is known in advance for the process and the tuned parameters of the ODOB controller satisfy the small gain theorem in (18), the robust stability of ODOB controller can be realized.

In this section, we will discuss robust stability analysis (one takes the thread p,t as an example) in the mixed product schedule for PB-EWMA, t-PCC, CF-EWMA and CPTDE controllers by using the small gain theorem and the mixed product ODOB control structure.

1) PB-EWMA:

If the thread p,t keeps on processing, the $\left\|Q_{p,t}\right\|_\infty$ of PB-EWMA can be calculated based on (3) as follows:

$$\left\|Q_{p,t}\right\|_\infty = \left\|\frac{\lambda_{p,t}}{z + \lambda_{p,t} - 1}\right\|_\infty \quad (20)$$

For the thread exchange (from other thread to the thread p,t), we can obtain the $\left\|Q_{c,p,t}\right\|_\infty$ according to (5) as follows:

$$\left\|Q_{c,p,t}\right\|_\infty = \left\|\frac{\lambda_{p,t}}{z^n + \lambda_{p,t} - 1}\right\|_\infty \quad (21)$$

As presented in the Appendix, it can be shown that $\left\|Q_{c,p,t}\right\|_\infty = \left\|Q_{p,t}\right\|_\infty$. Fig. 5 illustrates that the values

TABLE I

THE FILTER STRUCTURE RELATIONSHIPS AMONG PB-EWMA, T-PCC, CF-EWMA, CPTDE AND **Q** FILTER FOR THE THREAD p, t

Mixed product ODOB	PB-EWMA	CF-EWMA
$1^{st}\ Q_{p,t}(z)=\frac{1+a}{z+a}$	$a=\lambda_{p,t}-1$	$a=\lambda_{p,t}-1$
Mixed product ODOB	**t-PCC**	**CPTDE**
$2^{nd}\ Q_{p,t}(z)=\frac{(a_1+2)z+(a_2-1)}{z^2+a_1z+a_2}$	$a_1=-2+\lambda_{p,t}+w_{p,t}$ $a_2=1-\lambda_{p,t}-w_{p,t}+\lambda_{p,t}w_{p,t}$	$a_1=-2+\lambda_{p,t}+w_{p,t}$ $a_2=1-\lambda_{p,t}$

TABLE II

THE FILTER STRUCTURE RELATIONSHIPS AMONG PB-EWMA, T-PCC, CF-EWMA, CPTDE AND $\mathbf{Q_c}$ FILTER FOR THE THREAD p, t

Mixed product ODOB	PB-EWMA
$n^{th}\ Q_{c,p,t}(z)=\frac{1+a}{z^n+a}$	$a=\lambda_{p,t}-1$
Mixed product ODOB	**t-PCC**
$2n^{th}\ Q_{c,p,t}(z)=\frac{(a_1+2)z^n+(a_2-1)}{z^{2n}+a_1z^n+a_2}$	$a_1=-2+\lambda_{p,t}+w_{p,t}$ $a_2=1-\lambda_{p,t}-w_{p,t}+\lambda_{p,t}w_{p,t}$
Mixed product ODOB	**CF-EWMA**
$2n+m^{th}\ Q_{c,p,t}(z)=\frac{az(z^{m-1}-1)}{z^n[(z-1)z^{n+m-1}+(1-z+a)z^{m-1}-a]}$	$a=\frac{n\lambda_{p,t}}{m-1}$
Mixed product ODOB	**CPTDE**
$2n^{th}\ Q_{c,p,t}(z)=\frac{(a_1+2)z^n+(a_2-1)}{z^{2n}+a_1z^n+a_2}$	$a_1=-2+\lambda_{p,t}+nw_{p,t}$ $a_2=1-\lambda_{p,t}$

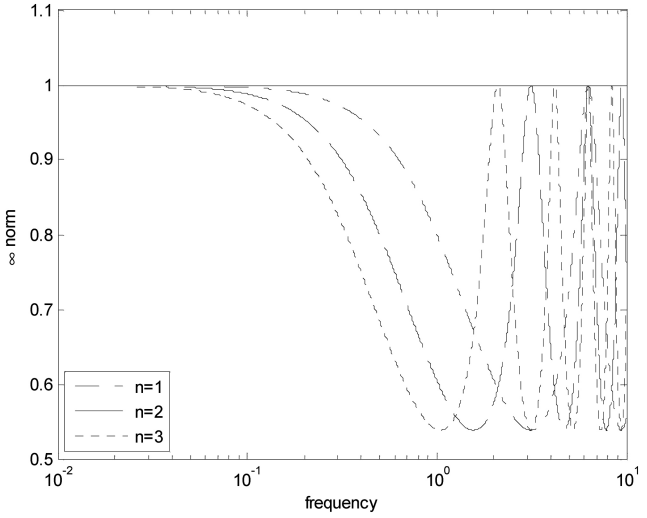

Fig. 5. $\left\|Q_{c,p,t}\right\|_\infty$ of PB-EWMA filter, $\lambda_{p,t}=0.7$.

of $\left\|\lambda_{p,t}/(z^n+\lambda_{p,t}-1)\right\|_\infty$ are equal for $n = 1, 2, 3$ and $\lambda_{p,t}=0.7$. According to (18)-(19), we have

$$\left\|\Delta_{p,t}\right\|_\infty \left\|\frac{\lambda_{p,t}}{b_{p,t}\left(z+\lambda_{p,t}-1\right)}\right\|_\infty \le 1 \tag{22}$$

If the uncertainty bound of thread p,t and the parameters of nominal plant $b_{p,t}$ are known in advance, the robust stability of ODOB controller can be realized when proper $\lambda_{p,t}$ satisfies (22).

2) t-PCC:

Based on (7) and (9), we can calculate the $\left\|Q_{p,t}\right\|_\infty$ and $\left\|Q_{c,p,t}\right\|_\infty$ of t-PCC as follows:

$$\left\|Q_{p,t}\right\|_\infty = \left\|\frac{\left(\lambda_{p,t}+w_{p,t}\right)z-\lambda_{p,t}-w_{p,t}-\lambda_{p,t}w_{p,t}}{z^2+\left(\lambda_{p,t}+w_{p,t}-2\right)z+1-\lambda_{p,t}-w_{p,t}-\lambda_{p,t}w_{p,t}}\right\|_\infty \tag{23}$$

$$\left\|Q_{c,p,t}\right\|_\infty = \left\|\frac{\left(\lambda_{p,t}+w_{p,t}\right)z^n-\lambda_{p,t}-w_{p,t}+\lambda_{p,t}w_{p,t}}{z^{2n}+\left(\lambda_{p,t}+w_{p,t}-2\right)z^n+1-\lambda_{p,t}-w_{p,t}+\lambda_{p,t}w_{p,t}}\right\|_\infty \tag{24}$$

It can also be shown that $\left\|Q_{c,p,t}\right\|_\infty = \left\|Q_{p,t}\right\|_\infty$, where the details are listed in Appendix. Fig. 6 demonstrates that the values of $\left\|Q_{c,p,t}\right\|_\infty$ are equal when $n = 1, 2, 3$,

Therefore we have

$$\left\|\Delta_{p,t}\right\|_\infty \left\|\frac{\left(\lambda_{p,t}+w_{p,t}\right)z-\lambda_{p,t}-w_{p,t}+\lambda_{p,t}w_{p,t}}{b_{p,t}[z^2+\left(\lambda_{p,t}+w_{p,t}-2\right)z+1-\lambda_{p,t}-w_{p,t}+\lambda_{p,t}w_{p,t}]}\right\|_\infty \le 1 \tag{25}$$

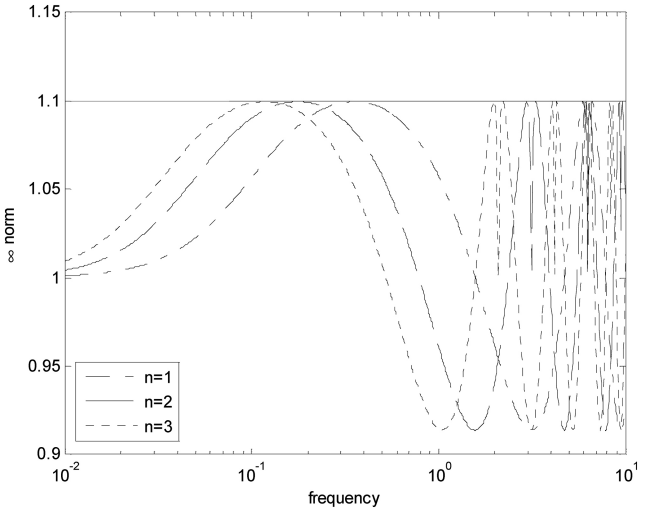

Fig. 6. $\left\|Q_{c,p,t}\right\|_\infty$ of t-PCC filter, $(\lambda_{p,t}, w_{p,t}) = (0.9, 0.1)$.

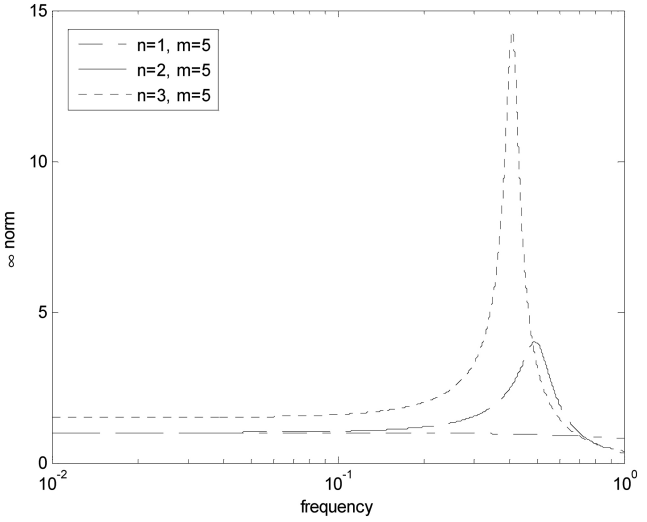

Fig. 7. $\left\|Q_{c,p,t}\right\|_\infty$ of CF-EWMA filter, $\lambda_{p,t} = 0.7$.

If the uncertainty bound of thread *p,t* and the parameters of nominal plant $b_{p,t}$ are known in advance, the robust stability of ODOB controller can be realized when proper $\lambda_{p,t}$ and $w_{p,t}$satisfy (25).

3) CF-EWMA:

From (10) and (12), we can calculate the $\left\|Q_{p,t}\right\|_\infty$ and $\left\|Q_{c,p,t}\right\|_\infty$ of CF-EWMA as follows:

$$\left\|Q_{p,t}\right\|_\infty = \left\|\frac{\lambda_{p,t}}{z+\lambda_{p,t}-1}\right\|_\infty \tag{26}$$

$$\left\|Q_{c,p,t}\right\|_\infty = \left\|\frac{\psi_{p,t}\left(z^{m-1}+z^{m-2}+\cdots+z\right)}{z^n\left[z^{n+m-1}-z^{m-1}+\psi_{p,t}\left(z^{m-2}+z^{m-3}+\cdots+1\right)\right]}\right\|_\infty \tag{27}$$

Equation (26) shows that the $\left\|Q_{p,t}\right\|_\infty$ is the same as PB-EWMA case when the same thread keeps on processing; however, the $\left\|Q_{c,p,t}\right\|_\infty$ is various depending on the values of n and m when the process thread is exchanged. Fig. 7 shows that the value of $\left\|Q_{c,p,t}\right\|_\infty$ are various for $\lambda_{p,t} = 0.7$, $m = 5$, $n = 1, 2, 3$.

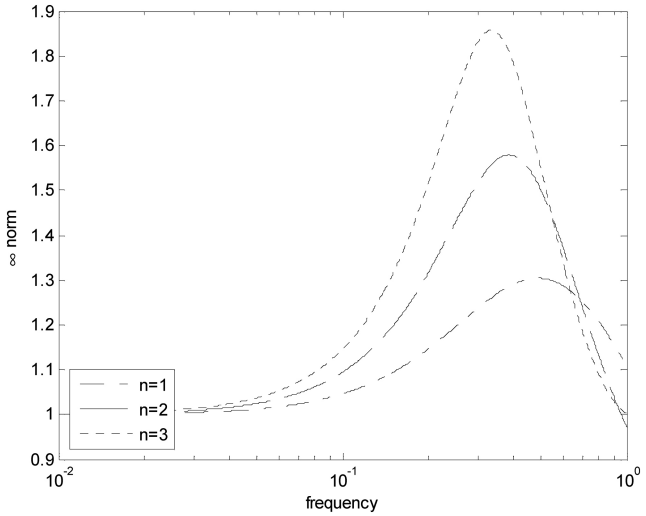

Fig. 8. $\left\|Q_{c,p,t}\right\|_\infty$ of CPTDE filter, $(\lambda_{p,t}, w_{p,t}) = (0.7, 0.2)$.

4)CPTDE:

The $\left\|Q_{p,t}\right\|_\infty$ and $\left\|Q_{c,p,t}\right\|_\infty$ of CPTDE can be obtained from (14) and (16) as follows:

$$\left\|Q_{p,t}\right\|_\infty = \left\|\frac{\left(\lambda_{p,t}+w_{p,t}\right)z-\lambda_{p,t}}{z^2+\left(\lambda_{p,t}+w_{p,t}-2\right)z+1-\lambda_{p,t}}\right\|_\infty \tag{28}$$

$$\left\|Q_{c,p,t}\right\|_\infty = \left\|\frac{\left(\lambda_{p,t}+nw_{p,t}\right)z^n-\lambda_{p,t}}{z^{2n}+\left(\lambda_{p,t}+nw_{p,t}-2\right)z^n+\left(1-\lambda_{p,t}\right)}\right\|_\infty \tag{29}$$

Equation (28) shows that the $\left\|Q_{p,t}\right\|_\infty$ is a constant if the tuned parameters $\lambda_{p,t}$and $w_{p,t}$are given when the same thread keeps on processing; however, the $\left\|Q_{c,p,t}\right\|_\infty$ is various depending on the break run number n when the process thread is exchanged. Fig. 8 shows that the values of $\left\|Q_{c,p,t}\right\|_\infty$ are different when break run number n is getting larger where $(\lambda_{p,t}, w_{p,t}) = (0.7, 0.2)$, $n = 1, 2, 3$.

The robust stability region of the PB-EWMA and t-PCC are easily to be obtained since $\left\|Q_{p,t}\right\|_\infty = \left\|Q_{c,p,t}\right\|_\infty$. For the cases of CF-EWMA and CPTDE, the exact robust stability region is hard to obtain. The values of $\left\|Q_{c,p,t}\right\|_\infty$ are various with the break run numbers, n, or the number of the thread *p,t* at the last production cycle, m, because the initial compensation scheme considers the information on the break run and the previous same thread when the threads is exchanged. For the practical mixed product manufacturing processes, the same thread is rarely exchanged immediately. Consequently, since $\left\|Q_{c,p,t}\right\|_\infty$is only used for the first transient run when the process thread has been exchanged, if it is assumed that the same process thread keeps on processing for several runs before it is changed to other thread, the difficulty can be avoided by just using $\left\|Q_{p,t}\right\|_\infty$to calculate the robust stability region.

IV. Optimal Performance of the Mixed Product ODOB

In the previously section, we introduced robust stability analysis by satisfying small gain theorem. If the boundary of

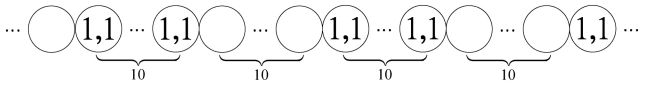

Fig. 9. The periodic mixed product schedule.

the model uncertainty $\|\Delta\|_\infty = \gamma$ is known in advance, the robust stable condition is $\left\|-\mathbf{b}^{-1}\mathbf{Q}\right\|_\infty \leq \frac{1}{\gamma}$ and can be rewritten as $\|\mathbf{Q}\|_\infty \leq \frac{1}{\left\|-\mathbf{b}^{-1}\right\|_\infty \cdot \gamma}$. On the other hand, if $\|\mathbf{Q}\|_\infty = \varepsilon$ for any positive ε is known in advance, the tolerance for the modeling uncertainty is $\|\Delta\|_\infty \leq \frac{1}{\left\|-\mathbf{b}^{-1}\right\|_\infty \cdot \varepsilon}$. There are lots of combinations of the tuned parameters which satisfy the robust stable constraints of the closed-loop system. In this section, one will apply the method [7], which tunes the parameters of the ODOB controller for guaranteeing the optimal nominal performance under the robust stability. Here, we study the cases of DT and ARIMA(1,1,1) with drift disturbances under periodic mixed product schedule as shown in Fig. 9. For the other disturbance structure like (IMA(1,1), random walk with drift and ARMA(1,1)), the optimal parameters of the mixed product ODOB can also be obtained by the same procedure. Each production period in Fig. 9 includes twenty runs (ten for thread 1,1 and ten for break products), and the target of thread 1,1 is set to zero.

In order to facilitate the optimal performance analysis, one makes two assumptions: The first one is that the same thread reaches steady state for several runs before it is exchanged. The second one is that the output error in the first transient run is calculated using $Q_{p,t}$instead of $Q_{c,p,t}$. The simulation results illustrate the assumptions is reasonable. As will be shown later, it shows that if the same thread lasts for five runs, the first assumption is fulfilled, and the error induced in the first transient run using $Q_{p,t}$is small as demonstrated in Section V. Nevertheless, if the assumptions are not satisfied, the approach provides the sub-optimal solution under stability condition.

A. Deterministic trend (DT) disturbance

Consider the DT disturbance, $\eta_k - \eta_{k-1} = \varepsilon_k - \varepsilon_{k-1} + \delta$, the z-transform is obtained as $H(z) = \frac{z-1}{z-1}\varepsilon(z) + \frac{\delta z}{(z-1)^2}$, where ε_k is independent identically distributed random variable and $\varepsilon_k \sim N\left(0, \sigma^2\right)$, δ denotes the constant increment of each run and $\varepsilon(z)$ denotes the z-transform of the white noise sequence. Appling Lee's method [7], the process output's sum square error (SSE) equation is derived as

$$\sum_{k=0}^{n} e_k^2 \cong \sum_{k=0}^{\infty} e_k^2 = \frac{2\left[-3 - a_1 + a_2\right]\sigma^2}{(a_2 - 1)(1 - a_1 + a_2)}$$

$$+\frac{\delta^2 (a_2 + 1)}{(1 - a_2)(1 + a_2 - a_1)(1 + a_2 + a_1)} \tag{30}$$

Suppose the benchmark $b = \beta = 1$ and $\left(\delta, \sigma^2\right) = (1, 1)$. Fig. 10 shows the contours of $\sum e^2(a_1, a_2)$ and $\|Q(a_1, a_2)\|_\infty$, respectively. If the tolerance of model uncertainty is $\frac{2}{3}$, i.e. $\|\Delta\|_\infty \leq \frac{2}{3}$ and then $\|Q\|_\infty = 1.5$, the optimum solution can be solved as $\mathbf{X}^* = \left(a_1^*, a_2^*\right) = (-0.752, 0.1673)$, i.e.

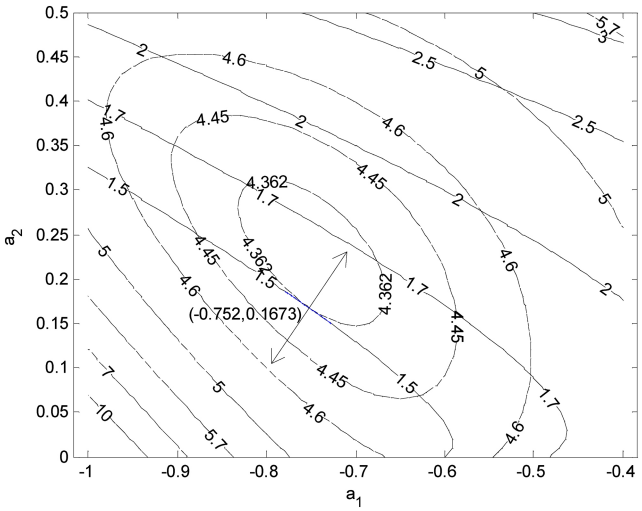

Fig. 10. Contours of SSE equation (dash line) and $\|Q\|_\infty$ (solid line) under DT disturbance.

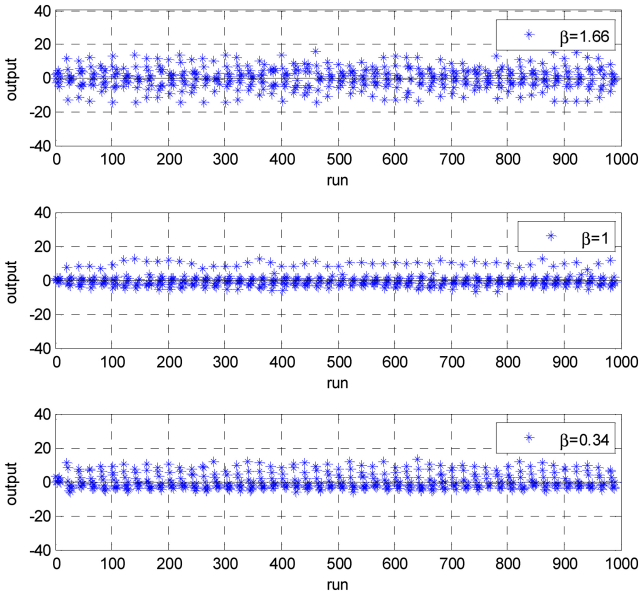

Fig. 11. Process outputs for DT disturbance with the parameters $(a_1, a_2) = (-0.752, 0.1673)$.

$\|Q(z)\|_\infty = \left\|\frac{1.248z - 0.8327}{z^2 - 0.752z + 0.1673}\right\|_\infty = 1.5$. While mapping the ODOB into the t-PCC controller one obtained $(\lambda, w) = (0.624 \pm j0.161, 0.624 \mp j0.161)$, but the complex weights of t-PCC controllers are never used in t-PCC controller. Therefore, it is shown that the parameter set of second-order ODOB control structure is larger than that of the t-PCC. Fig. 11 shows the simulation of the process output where the nominal plant is set $b = 1$ and the actual plants are $\beta = 0.34$, $\beta = 1$ and $\beta = 1.66$, respectively, corresponding to $\|\Delta\|_\infty \leq \frac{2}{3}$.

B. ARIMA(1,1,1) with drift disturbance

Consider the ARIMA(1,1,1) with drift disturbance, $\eta_k - (1 + \phi)\eta_{k-1} + \phi\eta_{k-2} = \varepsilon_k - \theta\varepsilon_{k-1} + \delta$, the z-transform is obtained

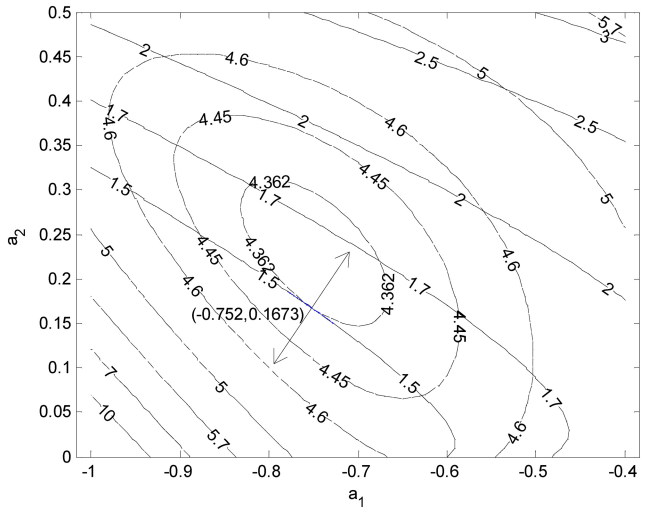

Fig. 12. Contours of SSE equation (dash line) and $\|Q\|_\infty$ (solid line) under ARIMA(1,1,1) with drift disturbance.

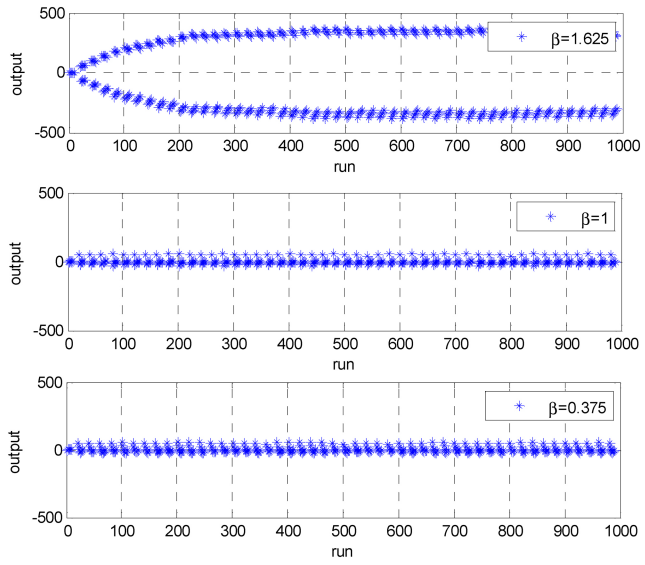

Fig. 13. Process output for ARIMA(1,1,1) with drift disturbance with the parameters $(a_1, a_2) = (-0.526, 0.03)$.

as $H(z) = \frac{z(z-\theta)}{(z-\phi)(z-1)}\varepsilon(z) + \frac{\delta z}{(z-1)^2}$. The SSE equation is derived as

$$\sum_{k=0}^{n} e_k^2 \cong \sum_{k=0}^{\infty} e_k^2 = \frac{2\sigma^2\left[1+\phi a_2+\theta\left(1+a_1-a_2-\phi+\phi a_1+\phi a_2\right)+\theta^2\left(1+\phi^2\right)\right]}{\left(1-a_1+a_2\right)\left(1-a_2\right)\left(1+\phi\right)\left(1+\phi a_1+\phi^2 a_2\right)} + \frac{\delta^2\left(a_2+1\right)}{\left(1-a_2\right)\left(1+a_2-a_1\right)\left(1+a_2+a_1\right)} \tag{31}$$

Suppose the benchmark $b = \beta = 1$ and $\left(\theta, \phi, \delta, \sigma^2\right) = (0.7, 0.8, 1, 1)$. Fig. 12 shows the contours of $\sum e^2(a_1, a_2)$ and $\|Q(a_1, a_2)\|_\infty$, respectively. If the tolerance of model uncertainty is 0.625, i.e. $\|\Delta\|_\infty \leq 0.625$ and then $\|Q\|_\infty = 1.6$, the optimum solution can be solved as $\mathbf{X}^* = \left(a_1^*, a_2^*\right) = (-0.526, 0.03)$, i.e. $\|Q(z)\|_\infty = \left\|\frac{1.474z-0.97}{z^2-0.526z+0.03}\right\|_\infty = 1.6$. While mapping the ODOB into

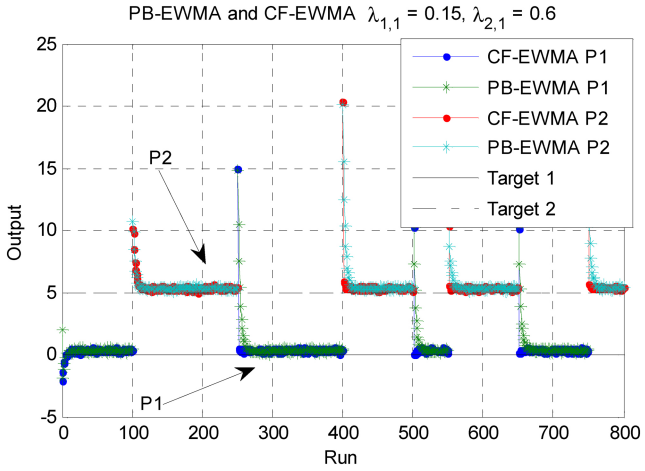

Fig. 14. The processes outputs with $\lambda_{1,1} = 0.15$ and $\lambda_{2,1} = 0.6$.

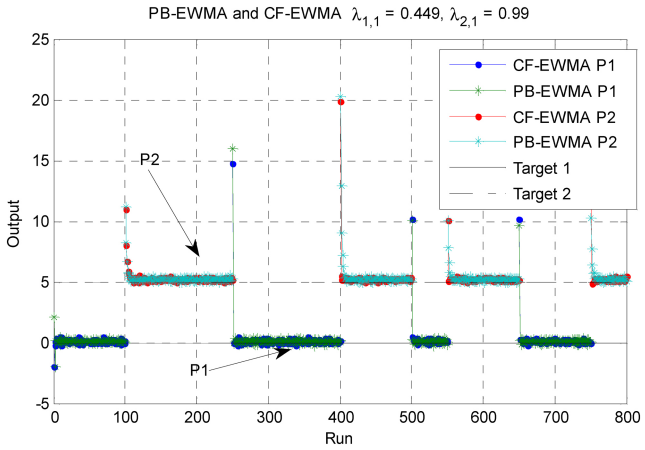

Fig. 15. The processes outputs with $\lambda_{1,1} = 0.499$ and $\lambda_{2,1} = 0.99$.

the t-PCC controller one obtained $(\lambda, w) = (0.934, 0.546)$. Fig. 13 shows the simulation of the process output where the nominal plant is set $b = 1$ and the actual plants are $\beta = 0.375$, $\beta = 1$ and $\beta = 1.625$, respectively corresponding to $\|\Delta\|_\infty \leq 0.625$. The uncertainty level for $\beta = 1.625$ makes the system approaching marginally stable state with a negative real pole, (-0.98, 0), which is also close to Nyquist frequency (-1, 0) (i.e., two points per cycle). Therefore, the response exhibits an oscillatory behavior but is still stable.

V. Case Study from the Literature

In this section, the PB-EWMA, t-PCC, CF-EWMA and CPTDE control schemes are compared using the simulation cases of periodic schedule production provided by Ai et al. [12] and Lee et al. [14]. There are one tool, two products and four cycles processes under IMA (1,1) with drift disturbance. The drift and moving average parameters are $\delta = 0.1$ and $\theta = 0.7$, while the white noise are sequences with zero mean and 0.01 variance, $\varepsilon \sim N(0, 0.1^2)$. The numbers of product 1 and product 2 for each cycle are [100,150], [150,100], [50,100] and [100,50]. The model mismatches for product 1 and product 2 are $[\xi_1, \xi_2] = [2,0.5]$; the actual parameters of the processes and the initial values of these four control schemes are: $[b_1, \beta_1] = [1,2]$ and $[b_2, \beta_2] = [1,0.5]$,

TABLE III
THE WEIGHTS FROM THE LITERATURE AND OPTIMAL WEIGHTS FOR THE CASE

PB-EWMA	Weights of [12]	ODOB
Product 1	$\lambda = 0.15$	$\lambda = 0.449$
Product 2	$\lambda = 0.6$	$\lambda = 0.99$
t-PCC	Weights of [14]	ODOB
Product 1	$\lambda_1 = 0.49,\ \lambda_2 = 0.01$	$\lambda_1 = 0.41,\ \lambda_2 = 0.01$
Product 2	$\lambda_1 = 0.99,\ \lambda_2 = 0.01$	$\lambda_1 = 0.99,\ \lambda_2 = 0.11$
CF-EWMA	Weights of [12]	ODOB
Product 1	$\lambda = 0.15$	$\lambda = 0.449$
Product 2	$\lambda = 0.6$	$\lambda = 0.99$
CPTDE	Weights of [14]	ODOB
Product 1	$\lambda_1 = 0.35,\ \lambda_2 = 0.01$	$\lambda_1 = 0.42,\ \lambda_2 = 0.01$
Product 2	$\lambda_1 = 0.99,\ \lambda_2 = 0.01$	$\lambda_1 = 0.99,\ \lambda_2 = 0.11$

TABLE IV
THE MSE OF SYSTEM OUTPUTS

PB-EWMA	Weights of [12]	ODOB	Improvement
Product 1	2.6235	1.2164	53.63%
Product 2	2.3414	1.3595	41.93%
t-PCC	Weights of [14]	ODOB	
Product 1	1.0889	1.0737	1.39%
Product 2	1.3126	1.2986	1.06%
CF-EWMA	Weights of [12]	ODOB	
Product 1	1.2300	1.1684	5.00%
Product 2	1.4533	1.2086	16.83%
CPTDE	Weights of [14]	ODOB	
Product 1	0.0294	0.0287	2.38%
Product 2	0.1574	0.1562	0.76%

which are the process gain and model gain for product 1 and product 2, respectively; $[\alpha_{1,0},\ \alpha_{2,0}] = [2,1]$, the actual intercept for product 1 and product 2, respectively; $[\hat{a}_{1,0},\ \hat{a}_{2,0}] = [2,1]$, the estimated intercept for product 1 and product 2, respectively, and $[\hat{d}_{1,0}, \hat{d}_{2,0}] = [0, 0]$, the initial value of drift term for product 1 and product 2, respectively. The output targets for products are $[T_1, T_2] = [0, 5]$. Noted that the weights of PB-EWMA and CF-EWMA are adopted from the simulation example of [12], and the weights of t-PCC and CPTDE are obtained from the simulation case of [14]. One takes the PB-EWMA case as an example to demonstrate the procedure of obtaining the optimal parameters by mixed product ODOB. With the system parameters and disturbance as mentioned above, we can compute the SSE equation with model mismatch for the first order ODOB as follows:

$$\sum_{k=0}^{n} e_k^2 \cong \sum_{k=0}^{\infty} e_k^2 = \frac{1 + 2(1+a)\xi - 2\theta\xi[1-(1+a)\xi] + \theta^2}{(1+a)\xi[2-(1+a)\xi]}\sigma^2 + \frac{\delta^2}{(1+a)^2\xi^2} \tag{32}$$

Since only one tuned parameter is involved, it is not necessary to plot the contour map of SSE equation but instead just to calculate the minimum of SSE in terms of a, or

$$\frac{\partial SSE}{\partial a} = 0$$
$$(1+a)\xi\left[(\xi+a\xi-1)(-1+\theta)^2 + (1+a)^2(1+\theta)^2\right]\sigma^2 - (-2+\xi+a\xi)^2\delta^2 = 0 \tag{33}$$

The optimal parameter for product 1 and product 2 can be obtained by (33). For the product 1 and product 2, the optimal parameter a and the corresponding weights of PB-EWMA and CF-EWMA filter are $(a_{1,1}, \lambda_{1,1}) = (0.7933, 0.99)$ and $(a_{2,1}, \lambda_{2,1}) = (-0.5516, 0.449)$, respectively. It is noted that the weights of PB-EWMA and CF-EWMA should follow the stability condition, i.e., $0 < \lambda \leq 1$. Fig. 14 shows the processes outputs of PB-EWMA and CF-EWMA controllers where the weights are $(\lambda_{1,1}, \lambda_{2,1}) = (0.15, 0.6)$ in [12]. Fig. 15 gives the

processes outputs of PB-EWMA and CF-EWMA controllers using the optimal parameters, $(\lambda_{1,1}, \lambda_{2,1}) = (0.449, 0.99)$. For the t-PCC and CPTDE, one can also calculate the optimal parameters by the same procedure as mentioned in Section IV. Table III lists the original weights in the literature and the optimal weights for these four mixed product control schemes. As compared the output performances of PB-EWMA with CF-EWMA controllers in Figs. 14 and 15, it is observed that the influence of $\|Q_c\|_\infty$ of CF-EWMA for the first run is not remarkable when the thread is exchanged. Also, it is observed that the output almost reaches steady state after five runs. The MSE results are listed in Table IV. It shows that the MSE of these four mixed product controllers are improved by using the optimal parameters and interestingly, also shows that the CPTDE scheme is the best one among all for this case. Compared with the second best one, t-PCC, the superiority of CPTDE scheme comes from the fact that the drift is compensated when the thread is exchanged.

VI. Conclusion

In this paper, we provided a unified framework of the mixed product RtR controllers, the mixed product ODOB control structure. The robust stability of the typical mixed product RtR controllers can be analyzed systematically by using mixed product ODOB control structure under mild assumptions. Furthermore, we provide a method for obtaining the optimal parameters which guarantee the optimal performance for the nominal plant under the robust stability. The simulation cases show that the output performance of PB-EWMA, t-PCC, CF-EWMA and CPTDE controllers is improved as compared to the one from literature by our method.

Appendix

PB-EWMA:

For the thread *p,t* keeping on processing, the $\left\|Q_{p,t}\right\|_\infty$ can be calculated as

$$\begin{aligned}\left\|Q_{p,t}\right\|_\infty &= \left\|\frac{\lambda_{p,t}}{z+\lambda_{p,t}-1}\right\|_\infty = \max_{0<\omega<\infty}\left|\frac{\lambda_{p,t}}{e^{j\omega}+\lambda_{p,t}-1}\right| \\ &= \frac{\lambda_{p,t}}{\min\limits_{0\le\omega<\infty}\left|e^{j\omega}\right|+\lambda_{p,t}-1}\end{aligned} \tag{A.1}$$

When thread is exchanged:

$$\begin{aligned}\left\|Q_{c,p,t}\right\|_\infty &= \left\|\frac{\lambda_{p,t}}{z^n+\lambda_{p,t}-1}\right\|_\infty = \max_{0<\omega<\infty}\left|\frac{\lambda_{p,t}}{e^{nj\omega}+\lambda_{p,t}-1}\right| \\ &= \frac{\lambda_{p,t}}{\min\limits_{0\le\omega<\infty}\left|e^{nj\omega}\right|+\lambda_{p,t}-1}\end{aligned} \tag{A.2}$$

where ω is frequency. According to equations (A.1)-(A.2), we have

$$\begin{cases}\min\limits_{0\le\omega<\infty}\left|e^{nj\omega}\right| = \min\limits_{0\le\omega<\infty}\left|\cos n\omega + j\sin n\omega\right| \\ = \min\limits_{0\le\omega<\infty}\sqrt{\cos^2 n\omega+\sin^2 n\omega}=1 \\ \min\limits_{0\le\omega<\infty}\left|e^{j\omega}\right| = \min\limits_{0\le\omega<\infty}\left|\cos\omega+j\sin\omega\right| = \min\limits_{0\le\omega<\infty}\sqrt{\cos^2\omega+\sin^2\omega}=1\end{cases}$$

Hence,

$$\min_{0\le\omega<\infty}\left|e^{nj\omega}\right| = \min_{0\le\omega<\infty}\left|e^{j\omega}\right| \tag{A.3}$$

Combining equations (A.1)-(A.3), we have

$$\begin{aligned}&\left\|\frac{\lambda_{p,t}}{z+\lambda_{p,t}-1}\right\|_\infty = \left\|\frac{\lambda_{p,t}}{z^n+\lambda_{p,t}-1}\right\|_\infty \\ &\left\|Q_{p,t}\right\|_\infty = \left\|Q_{c,p,t}\right\|_\infty, \forall 0<\lambda_{p,t}\le 1\end{aligned} \tag{A.4}$$

t-PCC:

For the thread *p,t* keeping on processing:

$$\begin{aligned}&\left\|Q_{p,t}\right\|_\infty \\ &= \left\|\frac{\left(\lambda_{p,t}+w_{p,t}\right)z-\lambda_{p,t}-w_{p,t}-\lambda_{p,t}w_{p,t}}{z^2+\left(\lambda_{p,t}+w_{p,t}-2\right)z+1-\lambda_{p,t}-w_{p,t}-\lambda_{p,t}w_{p,t}}\right\|_\infty \\ &= \max_{0<\omega<\infty}\left|\frac{\left(\lambda_{p,t}+w_{p,t}\right)e^{j\omega}-\lambda_{p,t}-w_{p,t}-\lambda_{p,t}w_{p,t}}{e^{2j\omega}+\left(\lambda_{p,t}+w_{p,t}-2\right)e^{j\omega}+1-\lambda_{p,t}-w_{p,t}-\lambda_{p,t}w_{p,t}}\right| \\ &= \frac{\max\limits_{0<\omega<\infty}\left|e^{j\omega}\right|\left(\lambda_{p,t}+w_{p,t}\right)-\lambda_{p,t}-w_{p,t}-\lambda_{p,t}w_{p,t}}{\min\limits_{0<\omega<\infty}\left|e^{2j\omega}\right|+\left(\lambda_{p,t}+w_{p,t}-2\right)\cdot} \\ &\quad\frac{1}{\min\limits_{0<\omega<\infty}\left|e^{j\omega}\right|+1-\lambda_{p,t}-w_{p,t}-\lambda_{p,t}w_{p,t}}\end{aligned} \tag{A.5}$$

When thread is exchanged:

$$\begin{aligned}&\left\|Q_{c,p,t}\right\|_\infty \\ &= \left\|\frac{\left(\lambda_{p,t}+w_{p,t}\right)z^n-\lambda_{p,t}-w_{p,t}+\lambda_{p,t}w_{p,t}}{z^{2n}+\left(\lambda_{p,t}+w_{p,t}-2\right)z^n+1-\lambda_{p,t}-w_{p,t}+\lambda_{p,t}w_{p,t}}\right\|_\infty \\ &= \max_{0<\omega<\infty}\left|\frac{\left(\lambda_{p,t}+w_{p,t}\right)e^{nj\omega}-\lambda_{p,t}-w_{p,t}+\lambda_{p,t}w_{p,t}}{e^{2nj\omega}+\left(\lambda_{p,t}+w_{p,t}-2\right)e^{nj\omega}+1-\lambda_{p,t}-w_{p,t}+\lambda_{p,t}w_{p,t}}\right| \\ &= \frac{\max\limits_{0<\omega<\infty}\left|e^{nj\omega}\right|\left(\lambda_{p,t}+w_{p,t}\right)-\lambda_{p,t}-w_{p,t}+\lambda_{p,t}w_{p,t}}{\min\limits_{0<\omega<\infty}\left|e^{2nj\omega}\right|+\left(\lambda_{p,t}+w_{p,t}-2\right)\cdot} \\ &\quad\frac{1}{\min\limits_{0<\omega<\infty}\left|e^{nj\omega}\right|+1-\lambda_{p,t}-w_{p,t}+\lambda_{p,t}w_{p,t}}\end{aligned} \tag{A.6}$$

Based on the equations (A.5)-(A.6), we have

$$\begin{cases}\min\limits_{0\le\omega<\infty}\left|e^{2nj\omega}\right| = \min\limits_{0\le\omega<\infty}\left|\cos 2n\omega+j\sin 2n\omega\right| \\ \qquad = \min\limits_{0\le\omega<\infty}\sqrt{\cos^2 2n\omega+\sin^2 2n\omega}=1 \\ \min\limits_{0\le\omega<\infty}\left|e^{2j\omega}\right| = \min\limits_{0\le\omega<\infty}\left|\cos 2\omega+j\sin 2\omega\right| \\ = \min\limits_{0\le\omega<\infty}\sqrt{\cos^2 2\omega+\sin^2 2\omega}=1\end{cases}$$

$$\min_{0\le\omega<\infty}\left|e^{2nj\omega}\right| = \min_{0\le\omega<\infty}\left|e^{2j\omega}\right| \tag{A.7}$$

and

$$\begin{cases}\max\limits_{0\le\omega<\infty}\left|e^{nj\omega}\right| = \max\limits_{0\le\omega<\infty}\left|\cos n\omega+j\sin n\omega\right| \\ = \max\limits_{0\le\omega<\infty}\sqrt{\cos^2 n\omega+\sin^2 n\omega}=1 \\ \max\limits_{0\le\omega<\infty}\left|e^{j\omega}\right| = \max\limits_{0\le\omega<\infty}\left|\cos\omega+j\sin\omega\right| = \max\limits_{0\le\omega<\infty}\sqrt{\cos^2\omega+\sin^2\omega}=1\end{cases}$$

$$\min_{0\le\omega<\infty}\left|e^{nj\omega}\right| = \min_{0\le\omega<\infty}\left|e^{j\omega}\right| \tag{A.8}$$

Combining equations (A.3), (A.5)-(A.8), we have

$$\begin{aligned}&\left\|\frac{\left(\lambda_{p,t}+w_{p,t}\right)z^n-\lambda_{p,t}-w_{p,t}+\lambda_{p,t}w_{p,t}}{z^{2n}+\left(\lambda_{p,t}+w_{p,t}-2\right)z^n+1-\lambda_{p,t}-w_{p,t}+\lambda_{p,t}w_{p,t}}\right\|_\infty \\ &= \left\|\frac{\left(\lambda_{p,t}+w_{p,t}\right)z-\lambda_{p,t}-w_{p,t}+\lambda_{p,t}w_{p,t}}{z^2+\left(\lambda_{p,t}+w_{p,t}-2\right)z+1-\lambda_{p,t}-w_{p,t}+\lambda_{p,t}w_{p,t}}\right\|_\infty \\ &\left\|Q_{p,t}\right\|_\infty = \left\|Q_{c,p,t}\right\|_\infty, \forall 0<\lambda_{p,t}\le 1, 0<w_{p,t}\le 1\end{aligned} \tag{A.9}$$

REFERENCES

[1] G. E. P. Box and G. M. Jenkins, *Time Series Analysis: Forecasting and Control*. Englewood Cliffs, NJ, USA: Prentice Hall PTR, 1994.

[2] E. Sachs, A. Hu, and A. Ingolfsson, "Run by run process control: Combining SPC and feedback control," *IEEE Trans. Semicond. Manuf.*, vol. 8, no. 1, pp. 26–43, Feb. 1995.

[3] S. W. Butler and J. A. Stefani, "Supervisory run-to-run control of polysilicon gate etch using in situ ellipsometry," *IEEE Trans. Semicond. Manuf.*, vol. 7, no. 2, pp. 193–201, May 1994.

[4] A. Chen, and R. Guo, "Age-based double EWMA controller and its application to CMP processes," *IEEE Trans. Semicond. Manuf.*, vol. 14, no. 1, pp. 11–19, Feb. 2002.

[5] S. Adivikolanu and E. Zafiriou, "Extensions and performance/robustness tradeoffs of the EWMA run-to-run controller by using the internal model control structure," *IEEE Trans. Electron. Packag. Manuf.*, vol. 23, no. 1, pp. 56–68, Jan. 2000.

[6] E. D. Castillo, "Long run and transient analysis of a double EWMA feedback controller," *IIE Trans.*, vol. 31, no. 12. pp. 1157–1169, Dec. 1999.

[7] A. C. Lee, Y. R. Pan, and M. T. Hsieh, "Output disturbance observer structure applied to run-to-run control for semiconductor manufacturing," *IEEE Trans. Semicond. Manuf.*, vol. 24, no. 1, pp. 27–43, Feb. 2011.

[8] M.-D. Ma, C.-C. Chang, S.-S. Jang, and D. S.-H. Wong, "Mixed product run-to-run process control - An ANOVA model with ARIMA disturbance approach," *J. Process Control,* vol. 19, no. 4, pp. 604–614, Apr. 2009.

[9] S. K. Firth, W. J. Campbell, A. Toprac, and T. F. Edgar, "Just-in-time adaptive disturbance estimation for run-to-run control of semiconductor processes," *IEEE Trans. Semicond. Manuf.*, vol. 19, no. 3, pp. 298–315, Aug. 2006.

[10] Y. Zheng, Q.-H. Lin, D. S.-H. Wang, S.-S. Jang, and K. Hui, "Stability and performance analysis of mixed product run-to-run control," *J. Process Control,* vol. 16, no. 5, pp. 431–443, Jun. 2006.

[11] M. D. Ma, C. C. Chang, D. S. H. Wong, and S. S. Jang, "Threaded EWMA controller tuning and performance evaluation in a high-mixed system," *IEEE Trans. Semicond. Manuf.*, vol. 22, no. 4, pp. 507–511, Nov. 2009.

[12] B. Ai, Y. Zheng, Y. Wang, S.-S. Jang, and T. Song, "Cycle forecasting EWMA (CF-EWMA) approach for drift and fault in mixed-product run-to-run process," *J. Process Control*, vol. 20, no. 5, pp. 689–708, Jun. 2010.

[13] B. Ai, Y. Zheng, S.-S. Jang, Y. Wang, L. Ye, and C. Zhou, "The optimal drift-compensatory and fault tolerant approach for mixed-product run-to-run control," *J. Process Control,* vol. 19, no. 8, pp. 1401–1412, Sep. 2009.

[14] A. C. Lee, T. W. Kuo, and C. T. Ma, "Combined product and tool disturbance estimator for the mix-product process and its application to the removal rate estimation in CMP process" *Int. J. Precis. Eng. Manuf.*, vol. 13, no. 4, pp. 471–481, Apr. 2012.

[15] K. Zhou and J. C. Doyle, *Essentials of Robust Control*. Englewood Cliffs, NJ, USA: Prentice Hall, 1998.

An-Chen Lee received the B.S. and M.S. degrees in power mechanical engineering from National Tsing Hua University, Hsinchu, Taiwan, and the Ph.D. degree in mechanical engineering from the University of Wisconsin-Madison, Madison, WI, USA, in 1986.

He is designated as Chair Professor of National Chiao Tung University, Hsinchu, and currently a Professor with the Department of Mechanical Engineering. His current research interests are CNC machine tool control technology, magnetic bearing technology, rotor dynamic and control, and semiconductor manufacturing process control. Dr. Lee served as an Editorial Board member of *International Journal of Precision Engineering and Manufacturing*, Chinese Society of Mechanical Engineers. He is the recipient of National Science Committee (NSC) Excellent Research Award in 1991-1992, NSC Distinguished Research Award in 1993-1994, 1995-1996, and 1997-1998, NSC research fellow in 1999-2001, and 2002-2004, NSC research fellow Award in 2005, Chinese Society of Mechanical Engineers Distinguished Engineering Professor Award in 2001, Gold Medal Award, Inventor/New Product Exposition, Pittsburgh, USA, in 2010, Gold Medal Award, International Exhibition of Inventions of Geneva in 2011, Brown Medal Award, and the International Exhibition of Inventions of Geneva in 2012.

Jeng-Haur Horng received the B.S. degree in naval architecture and marine engineering, and the M.S. and Ph.D. degrees in mechanical engineering from the National Cheng Kung University, Tainan, Taiwan, in 1996. He is currently a Distinguished Professor with the Department of Power Mechanical Engineering, National Formosa University, Yunlin, Taiwan. His current research interests include tribology, microcontact mechanics, and contact temperature of mechanical parts.

Tzu-Wei Kuo received the B.S. and M.S. degrees in mechanical engineering from Chung Hua University, Hsinchu, Taiwan, in 2001 and 2005, respectively, and the Ph.D. degree in mechanical engineering from National Chiao Tung University, Hsinchu, in 2012. He is currently a Senior Engineer at Premtek International Inc., Hsinchu. His current research interests include run-to-run control and process control.

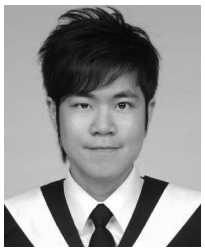

Nan-Hung Chou received the B.S. and M.S. degrees in mechanical engineering from National Chung Yuan University, Taoyuan, Taiwan, and National Chiao Tung University, Hsinchu, Taiwan, in 2009 and 2011, respectively. He is currently with the Taiwan Semiconductor Manufacturing Company, Taichung, Taiwan.